

Transpolar potential saturation: Roles of region 1 current system and solar wind ram pressure

G. L. Siscoe and N. U. Crooker

Center for Space Physics, Boston University, Boston, Massachusetts, USA

K. D. Siebert

Mission Research Corporation, Nashua, New Hampshire, USA

Received 14 November 2001; revised 22 May 2002; accepted 24 May 2002; published 23 October 2002.

[1] MHD simulations give about the same dependence of transpolar potential on solar wind electric field (IEF) as the Hill model of transpolar potential, including saturation and dependence on ram pressure. In the Hill model, feedback of the region 1 current system is presumed to limit the rate of reconnection at the magnetopause thereby causing transpolar potential saturation. MHD simulations add as relevant information that in the saturation domain the region 1 current system usurps the role of the Chapman-Ferraro current system, which disappears. This means that the region 1 current system takes on the role of providing the current and generating most of the magnetic field in the $\mathbf{J} \times \mathbf{B}$ force at the magnetopause that balances solar wind ram pressure. Viewed from this perspective, transpolar potential saturation results not from the region 1 current system limiting the rate of reconnection at the magnetopause but instead from ram pressure (more accurately, total solar wind stresses) limiting the total amount of current that can flow in the region 1 current system. Transpolar potential saturation is then the limit on transpolar potential that corresponds to the ram-pressure limit on total region 1 current. *INDEX TERMS:* 2784 Magnetospheric Physics: Solar wind/magnetosphere interactions; 2708 Magnetospheric Physics: Current systems (2409); 2776 Magnetospheric Physics: Polar cap phenomena; *KEYWORDS:* transpolar potential saturation, ram pressure

Citation: Siscoe, G. L., N. U. Crooker, and K. D. Siebert, Transpolar potential saturation: Roles of region 1 current system and solar wind ram pressure, *J. Geophys. Res.*, 107(A10), 1321, doi:10.1029/2001JA009176, 2002.

1. Introduction: Transpolar Potential Saturation

[2] Observations, theory, and modeling indicate that as the geoeffective component of the interplanetary electric field (IEF) increases from typical values, the electrical potential across the polar cap first increases linearly up to ~ 100 kV, then asymptotes to a limiting value that lies typically between 150 and 250 kV. The range from typical (~ 50 kV) to extreme (~ 250 kV) is about a factor of 5, while the corresponding range in IEF (from ~ 1 mV/m to ~ 50 mV/m) is ~ 50 . Thus the two quantities cannot be linearly related over their whole range of variation. The transpolar potential must level off above some value. Transpolar potential saturation, as this phenomenon is sometimes called, was explicitly noted by Reiff *et al.* [1981] and Wygant *et al.* [1983]. Reiff and Luhmann [1986] reviewed early observations of the effect. More recently, Russell *et al.* [2000, 2001] have presented examples in which transpolar potential saturation appears to be well illustrated. In statistical studies, in which there are in general few values of transpolar potential in the saturation regime, evidence of transpolar potential saturation appears as a nonlinearity setting in

around 100 kV [Burke *et al.*, 1999; Weimer, 2001]. The Russell *et al.* [2000, 2001] studies found that nonlinearity appears to set in when the IEF reaches ~ 3 mV/m.

[3] On the theoretical side, Hill [Hill *et al.*, 1976; Hill, 1984] predicted that the transpolar potential should saturate. He noted that magnetic reconnection at the magnetopause is subject to negative feedback from ionospheric currents to which it gives rise (region 1 currents [Iijima and Potemra, 1976]). He argued that the magnetic field that region 1 currents generate at the reconnection site should not exceed a significant fraction of Earth's dipole field there, since the two fields are oppositely directed and so tend to cancel. An upper limit on region 1 current implies an upper limit on transpolar potential. Consistent with this insight, Fedder and Lyon [1987] showed that in an MHD simulation ionospheric conductance indeed significantly modifies the shape of equipotentials in the magnetosphere in the sense of providing a negative feedback.

[4] Siscoe *et al.* [2002] gives an analytical formulation of the Hill model in which the magnetic field that region 1 currents generate at the magnetopause subsolar point (presumed to be the reconnection site) was calculated using a figure-8 current pattern (one loop for each hemisphere) lying in the dawn-dusk terminator plane. The resulting expression specifies transpolar potential as a function of

the IEF (the component that generates the reconnection potential at the magnetopause), solar wind ram pressure, ionospheric conductance, and geomagnetic dipole moment (to explore epochs with different dipole moments). They found that the dependence of the transpolar potential on ionospheric conductance and dipole moment predicted by the analytical formulation of the Hill model agrees quite well with results of MHD simulations. Other mentioned dependencies were not compared.

[5] Here we explicitly demonstrate that in MHD simulation the transpolar potential saturates as the IEF increases. We also compare the results of MHD simulation with the Hill model's prediction of the transpolar potential as a function of the IEF and ram pressure. We suggest that the reason that the transpolar potential saturates is that there is an upper limit on the total current in the region 1 current system set by the amount of current required to provide the $\mathbf{J} \times \mathbf{B}$ force needed to balance the solar wind ram pressure acting against the whole magnetosphere.

2. MHD Simulation

[6] For this study we have used the Integrated Space Weather Prediction Model (ISM), which is a global-magnetospheric MHD numerical code (for details see *White et al.* [2001]). The code integrates the standard MHD equations over a volume that extends from 40 R_e upwind from Earth to 300 R_e downwind and 60 R_e radially from an axis through Earth parallel to the solar wind flow direction. To treat the connection to the ionosphere the code uses a single set of equations from the base of the ionosphere to the outer boundaries of this grid. The single set of equations segues continuously from the ionosphere to the solar wind in the form of continuum mechanics equations appropriate to each domain. The numerical algorithm consists of a second order finite difference scheme with partial donor cell method (PDM) terms [*Hain*, 1987] to provide numerical stability in regions containing large gradients.

[7] Four ISM runs were made with $V = 500$ km/s, $n = 5$ protons/cm³, and $B_z = -2, -10, -20,$ and -30 nT. Here V , n , and B_z are solar wind speed, density, and z-component of the magnetic field, respectively. For simplicity the magnetic field was assumed to point straight south. These runs give the following range of IEF: 1, 5, 10, and 15 mV/m. The ram pressure in each case is 2 nPa. Ionospheric Pedersen conductance, which in the version of the code used in this study is uniform over the ionosphere (except for the inverse dependence on field strength), was taken to be 12 S at the pole. The grid spacing in the ionosphere was about 600 km. The Earth did not rotate in these simulations, Hall conductance was set to zero, and the dipole was perpendicular to the solar wind flow direction. The resulting potential pattern is symmetric in the dawn-dusk direction. Conditions were held steady for 2 hours after which values were obtained for the plots shown in section 4.

3. Hill Model

[8] The Hill model of transpolar potential assumes that for any IEF the transpolar potential (Φ_H where the subscript "H" denotes that this is the transpolar potential that the Hill model gives and so should perhaps be called the Hill

potential) is determined by the interplay between an unsaturated transmagnetospheric potential (Φ_M) and a saturated transpolar potential (Φ_S). Φ_M is the potential drop around the magnetopause that results from magnetic reconnection in the absence of the saturation mechanism. (For simplicity, viscous driving is ignored.) This is an idealized potential drop in that the model assumes that it increases linearly with IEF even into the saturation domain where, according to the model, the real reconnection potential drop is saturated. Φ_S is the transpolar potential that generates region 1 current strong enough to prevent any further increase in the reconnection rate by creating an opposing magnetic field at the reconnection site.

[9] To express the interplay between the potentials, Hill combined them as follows:

$$\Phi_H = \Phi_M \Phi_S / (\Phi_M + \Phi_S). \quad (1)$$

In the linear range of Φ_M , when $\Phi_M \ll \Phi_S$, Φ_S drops out of the relation, and $\Phi_H = \Phi_M$, as we normally assume. In the nonlinear range, when $\Phi_M \gg \Phi_S$, saturation at the value $\Phi_H = \Phi_S$ automatically results.

[10] As noted above, *Siscoe et al.* [2002] gives analytical expressions for Φ_M and Φ_S in terms of solar wind, ionospheric, and dipole parameters. The derivation of transmagnetospheric potential, Φ_M , is based on conventional magnetic reconnection theory applied to the magnetopause. It treats the aerodynamics of the solar wind interaction with the magnetosphere to find expressions for parameters that enter into the reconnection theory. The result is

$$\Phi_M(\text{kV}) = 57.6 \text{ IEF}(\text{mV/m}) p_{\text{sw}}(\text{nPa})^{-1/6}. \quad (2)$$

Here IEF is the solar wind motional electric field (VB where, for this study, the magnetic field is assumed to point straight south), and p_{sw} is the solar wind ram pressure (ρV^2 where ρ is solar wind mass density). The $-1/6$ exponent corresponds to the standard Chapman-Ferraro scaling relation for how the scale size of the magnetosphere depends on ram pressure. Equation (2) turns out to be similar to empirical formulas reviewed by *Reiff and Luhmann* [1986] in which the average of five values of the empirical slope of Φ_M versus IEF is 44.8, compared with 57.6 in equation (2). Taking the $p_{\text{sw}}^{-1/6}$ factor into account (since p_{sw} is typically around 2 nPa) brings the Reiff and Luhmann average value up to nearly the value given in equation (2). We appeal to this correspondence with observations in place of reviewing the original derivation of equation (2).

[11] The derivation of Φ_S is based on the magnetic field generated by the figure-8 current loop described above. Equation (3) gives an analytic formula for the strength of the magnetic field that this current loop generates at the stagnation point at the magnetopause

$$B_{1s} = 0.014 \mu_0 I_1 / R_E p_{\text{sw}}^{1/6}, \quad (3)$$

where I_1 and R_E are total region 1 current and radius of the Earth, respectively. To obtain this expression, we have taken the ratio of the radius of the region 1 loop to the distance to the stagnation point to be 3/2, which is consistent with

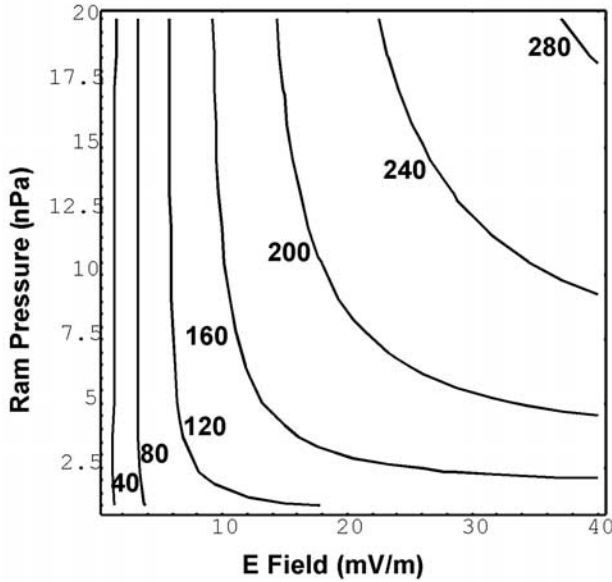


Figure 1. Contours of transpolar potential (in kV) as a function of solar wind ram pressure and interplanetary electric field (IEF). Plot based on the Hill model of transpolar potential saturation as formulated by *Siscoe et al.* [2002].

standard magnetospheric shape. In the spirit of the Hill model, we take the saturation region 1 current to be the value of I_1 that weakens the dipole field there by 50%. We choose the value 50% as an a priori unbiased value. Were we to use a value other than 50%, we would need to justify the choice with some additional consideration that lies outside the Hill model. (For example, *Siscoe et al.* [2002] use 41% to optimize the agreement between models.) Taking the distance to the stagnation point for $p_{sw} = 1$ nPa to be $10 R_e$ this gives

$$I_S(\text{MA}) = 5.6 p_{sw}(\text{nPa})^{1/3}. \quad (4)$$

One then finds the saturation transpolar potential, Φ_S , by use of an ionospheric Ohm's law in the form

$$I_S(\text{MA}) = \xi \Sigma(S) \Phi_S(\text{kV}) 10^{-3}, \quad (5)$$

where Σ is ionospheric conductance, and the coefficient ξ parameterizes the geometry of current flow lines in the ionosphere. As determined by global MHD simulations, ξ usually lies between 3 and 4. In the following, we take Σ to be 12 Siemens and $\xi = 3.6$, which is its average value in the four ISM runs mentioned earlier.

[12] Equations (1), (2), (4), and (5) can now be combined to give an expression for Φ_H as a function of IEF and p_{sw} that covers the full range from linear to saturation.

$$\Phi_H = 57.6 p_{sw}^{1/3} \text{IEF} / (p_{sw}^{1/2} + 0.01 \xi \Sigma \text{IEF}). \quad (6)$$

This expression for Φ_H is based on several idealizations among which we mention the following: (1) The Chapman-Ferraro scaling for the size of the magnetosphere introduced

in equation (2) ignores magnetospheric "erosion" that happens for southward IMF. (2) The region 1 current system is represented by two circular loops in the terminator plane, whereas the real currents are distributed sunward and tailward of the terminator plane and are not really circular. (3) The shape factor $3/2$ introduced in equation (3) ignores an increase in flaring angle of the flanks of the magnetosphere that happens for southward IMF. Thus equation (3) must be regarded as a zeroth order representation of the Hill potential suitable for revealing qualitative properties of the Hill model.

[13] Figure 1 summarizes the content of equation (6). One sees that in general the transpolar potential tends to be insensitive to ram pressure for low values of IEF and insensitive to the electric field for high values. (This is the saturation phenomenon.) It takes stronger IEF to saturate the potential for big ram pressures. Note also that for fixed IEF, transpolar potential increases with ram pressure. One can use this behavior to discriminate between the Hill model, in which the mechanism responsible for saturation depends on the total current flowing in the region 1 current system, and an alternative explanation in which the transpolar potential is proportional to the length of the reconnection line. In the latter case, transpolar potential might be expected to decrease as ram pressure increases for fixed IEF.

4. Comparison

[14] Figure 2 shows the transpolar potential obtained from the four MHD simulations described in section 2 and compares them with the Hill model as parameterized in section 3. In this case, $p_{sw} = 2$ nPa. The correspondence between values from the two models is quite good. Since we did not "tune" the parameters to optimize the fit, we should not be surprised that the agreement is not better. Also, as just mentioned, the formula is only an approximation. Nonetheless, parallel evolution toward saturation in both models is evident. It seems very likely then that the MHD simulation and the Hill model are employing essentially the same saturation mechanism, which in the Hill model is explicitly related to the region 1 current system. We may therefore ask the MHD simulation what aspect of the region 1 current system it is using to cause saturation of transpolar potential. As we discuss below, the answer it gives has more to do with ram pressure limiting the total current in the region 1 system than with limiting the total rate of reconnection, as one might otherwise assume.

[15] Given the central role that ram pressure plays in our interpretation of the cause of transpolar potential saturation, it is important before going further to verify that in MHD simulation the transpolar potential responds to changes in ram pressure in the way that the Hill model predicts. For this purpose we have rerun the $B_z = -20$ nT case with doubled density ($n = 10 \text{ cm}^{-3}$ instead of 5 cm^{-3}), which doubles the ram pressure (from 2.1 nPa to 4.2 nPa) but leaves the IEF unchanged (10 mV/m). Figure 3 shows the result. The transpolar potentials in the two runs are 144.4 kV for the lower ram pressure and 168.2 kV for the higher ram pressure, which verifies that the simulation behaves like the Hill model at least to the extent that the trend is the same as predicted by equation (6) (higher transpolar potential for higher ram pressure at fixed IEF).

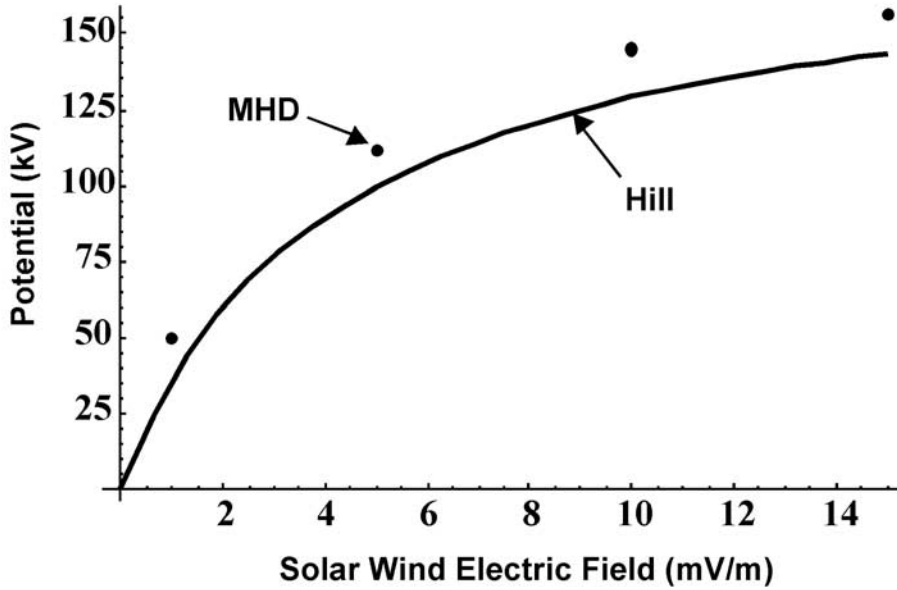


Figure 2. Comparison of MHD simulation (points) and Hill model (curve) showing transpolar potential saturation. (Solar wind ram pressure is 2 nPa.)

[16] To make the comparison quantitative, we compare the relative increase in potentials in the two models. The ratio of the transpolar potentials for the two MHD runs is $168.2/144.4 = 1.16$. Using equation (6) to represent the Hill model and taking $\xi = 3.6$ and $\Sigma = 12$ S (as in the MHD simulation) gives 1.14 for the ratio of the transpolar potentials for the two cases. The agreement is remarkably close

(1.14 versus 1.16) and serves to justify taking seriously the assumption that the MHD simulation and the Hill model use essentially the same physics to couple solar wind parameters to the transpolar potential. This is an important point because we know explicitly what physics is operating in the Hill model. The Hill model contains only two factors: reconnection at the magnetopause and the region 1 current

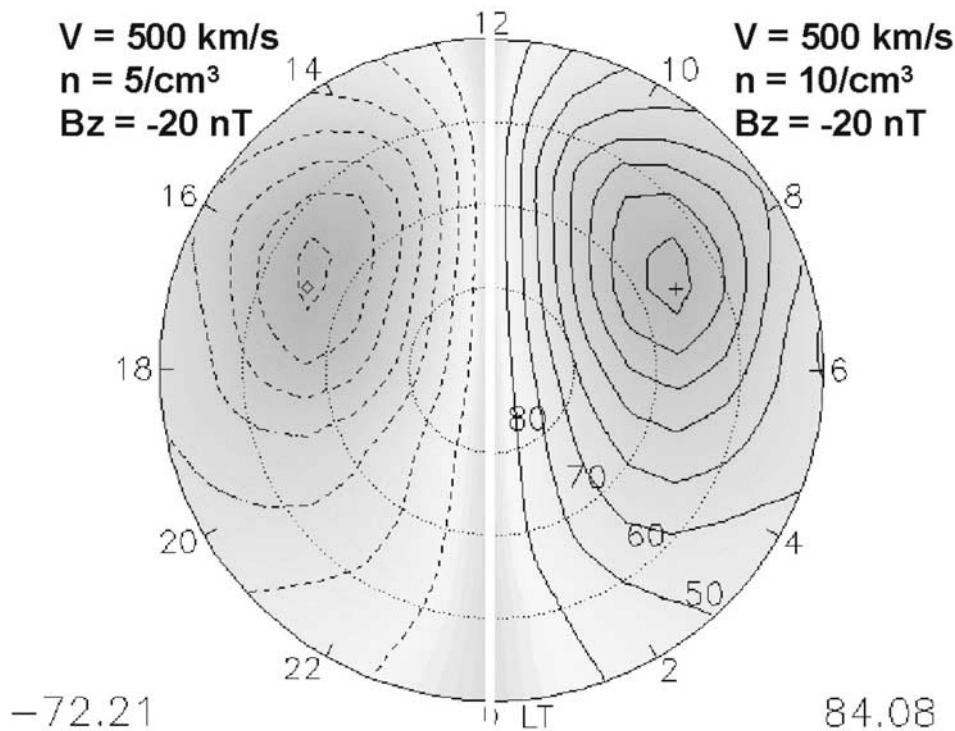


Figure 3. Equipotentials in polar cap for ram pressures 2.1 nPa (left) and 4.2 nPa (right) for the same IEF (10 mV/m).

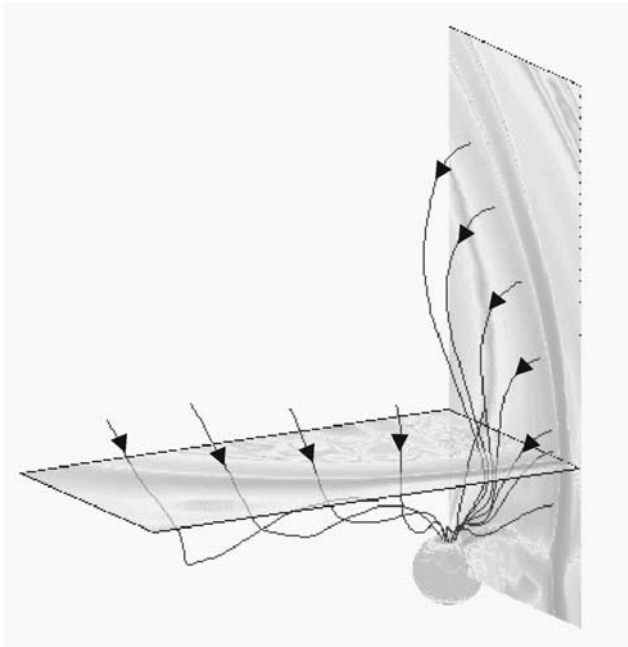


Figure 4. Three-dimensional view generated from the simulation having maximum IEF. Current flowlines were initiated in the tan layer, representing the magnetopause. Shading denotes radial component of the $\mathbf{J} \times \mathbf{B}$ force (tan is outward directed force and blue is inward directed force). See color version of this figure at back of this issue.

system. The first determines the transpolar potential in the unsaturated range of IEFs (this is just the standard relationship between reconnection at the magnetopause and the transpolar potential). The second factor, the region 1 current system, is responsible for causing saturation.

[17] Zesta *et al.* [2000] reports one instance in which region 1 current increased in response to a solar wind pressure pulse when the IMF was strongly southward. This author has subsequently used DMSP data to show directly that the transpolar potential increases in response to solar wind pressure pulses when the IMF points southward [E. Zesta, private communication, 2002].

5. How Ram Pressure (Not Reconnection) Might Limit Transpolar Potential

[18] Figure 4, which comes from the output of the $B_z = -30$ nT (IEF = 15 mV/m) ISM run, shows flowlines of electric current initiated at the magnetopause current that tell a surprising story. This is a three-dimensional (3-D) image seen from a northern-dawn viewpoint, with the Earth a partially hidden sphere at the bottom. There are two sets of current flowlines; in one of which, flowlines cross the noon-meridian plane (i.e., the xz plane) in a dawnward direction at the high-latitude dayside magnetopause then turn Earthward to follow the magnetic field into the dawnside polar cap. Flowlines in the other set cross a “horizontal” plane that floats $5 R_E$ above the equatorial plane (i.e., $z = 5 R_E$). Color shading on the meridian and horizontal planes reveals two current layers, the inner one of which (tan color) is the magnetopause. Colors denote the direction in which the $\mathbf{J} \times \mathbf{B}$ force pushes (tan for outward and blue for inward).

The magnetopause current layer pushes outward against the solar wind. The outer layer represents the ram force of the solar wind pushing inward.

[19] (Though it deflects us briefly from our message, we should point out the remarkably low height above the equatorial plane of the dayside cusp ($z \sim 2 R_E$ instead of a more typical $8 R_E$) and the unusual indenting of the nose of the magnetopause. These features look strange because we are not used to depicting or seeing the magnetosphere under such a strong southward IMF.)

[20] Current flowlines in Figure 4 were initiated along the ridge of maximum outward force in the inner (magnetopause) layer. Surprisingly, they turn out to be part of the region 1 current system. The little patch of tan color barely visible at the North Pole of Earth and into which all current flowlines converge marks the ionospheric location of the region 1 current. All current flowlines initiated in the inner layer above the cusp map into this patch. Thus where one expects the Chapman-Ferraro current system to be one finds instead the region 1 current system. There is no Chapman-Ferraro current above the cusp. Below the cusp, where one also expects to find the Chapman-Ferraro current, the magnetopause is occupied instead by a reconnection current system that closes mainly in the magnetosheath and on the bow shock [Siebert and Siscoe, 2002]. Thus the Chapman-Ferraro current system, characterized by closing on the magnetopause, is totally absent. We should note for its relevance to discussion below that whereas Figure 4 shows current flowlines closing through the magnetopause in the noon meridian plane, most of the current in the region 1 system closes (i.e., crosses from the dusk side to the dawn side) through the high-latitude magnetosheath and bow shock. This distributed mode of current closure happens because the MHD structure that effects the closure in this case is a combination of fast mode waves propagating out into the magnetosheath and slow mode waves propagating into the magnetosphere and tail [Coroniti and Kennel, 1979]. Under the condition of a strong southward IMF, the fast mode wave is very broad. (Incidentally, all current flowlines initiated in the outer, blue layer close in the magnetosheath.)

[21] As the IMF changes from northward to southward then to strongly southward (as here), the Chapman-Ferraro current does not suddenly disappear at some point. It gradually vanishes; its place being gradually usurped by currents of the region 1 and reconnection systems. (A similar situation in which the Chapman-Ferraro current disappears as the external magnetic field increased was reported by Crooker and Siscoe [1986] but in the context of vacuum superposition of fields.)

[22] In the saturation limit where there is no Chapman-Ferraro current, the region 1 current system acquires the dynamical role that under unsaturated conditions the Chapman-Ferraro current plays. It provides the $\mathbf{J} \times \mathbf{B}$ force needed to hold off the solar wind ram pressure, as Figure 4 with its inward and outward $\mathbf{J} \times \mathbf{B}$ shading illustrates. Although the region 1 current system takes on the force-providing role only above the cusp, this area covers most of the dayside magnetopause since under a condition of transpolar potential saturation the cusp at the magnetopause is at low latitude.

[23] We can now see how it is that instead of a limit on reconnection rate, ram pressure might cause transpolar

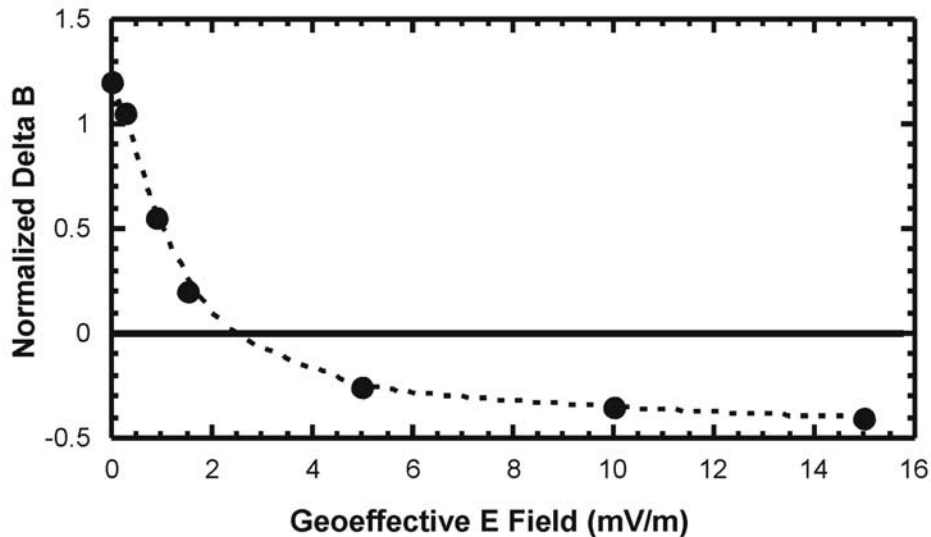


Figure 5. Ordinate is excess magnetospheric magnetic field strength relative to dipole field strength at the subsolar magnetopause normalized to dipole field strength. Abscissa is the component of solar wind electric field parallel to magnetic merging line on the magnetopause.

potential saturation. The pure Chapman-Ferraro situation with no region 1 current serves as a paradigm case for this discussion. The idealized Chapman-Ferraro problem (find the shape of the boundary formed by solar wind ions specularly reflecting off a magnetically closed magnetopause comprised solely of Chapman-Ferraro current) was solved in the 1960s. It gives a simple expression for the value for the total current needed to stop and deflect the solar wind, the product of the stagnation field strength and the “vertical” distance to the cusp divided by μ_0 . For a ram pressure of 2 nPa (the value used in the four simulations for this study), the answer is ~ 3.5 MA. Despite its being a product of idealizing assumptions this number, 3.5 MA, gives a rough measure of the strength of the interaction between the solar wind and the magnetosphere, not just what it happens to be but also what it can be.

[24] The last comment is important for it states the principle of interaction current limitation, which we suggest underlies the phenomenon of transpolar potential saturation. Since in the saturation domain, current flowing in the region 1 current system becomes the interaction current, it has a cap that it cannot exceed, and this in turn means a limit on transpolar potential. The principle of interaction current limitation can be argued more generally from dimensional analysis. The total force that the solar wind exerts on the magnetosphere (the so-called wave drag in aerodynamic parlance) can be written dimensionally as $R_E^2 L^2 p_{sw}$, where L is a characteristic width of the magnetosphere in units of R_E and p_{sw} is solar wind ram pressure ($\sim \rho V^2$). This same total force can also be expressed dimensionally in terms of the total force-related current (I_f) and the force-related magnetic field strength (B_{st}) as $R_E L I_f B_{st}$. The force-related magnetic field is dimensionally related to the ram pressure by $B_{st} = (2\mu_0 p_{sw})^{1/2}$, and the scale length L is dimensionally related to the dipole field B_o at the Earth’s surface by $L = (B_o/B_{st})^{1/3}$. Combining these gives a characteristic value for the force-related interaction current: $I_f = R_E (B_o B_{st}^2)^{1/3} / \mu_0$. This value

depends only on the solar wind ram pressure through B_{st} . For a ram pressure of 2 nPa the value is $I_f = 2.7$ MA, which is gratifyingly close to the 3.5 MA given above for the Chapman-Ferraro current.

[25] The component of the interaction current that we have just considered, I_f , refers to the “push” that the solar wind exerts on the magnetosphere or the normal stress in the language of continuum mechanics. The solar wind also exerts a “pull,” or tangential stress. The tangential stress creates the magnetotail. To shear the magnetically reconnected field from its interplanetary orientation to its tail orientation requires parallel current. After the current shears the field parallel to the solar wind flow, the interaction stops. Thus 90° shear gives an upper limit on this component of the interaction current. The MHD simulations that we have been discussing indicate that in the saturation domain, the parallel current associated with shearing the interplanetary magnetic field (B_{sw}) from a southward orientation into a Sunward (or antiSunward) direction constitutes a significant second component of the region 1 current system. A dimensional analysis of this component (I_s) is relatively straightforward: $I_s = 2R_E L B_{sw} / \mu_0$. The factor of $\sqrt{2}$ seems appropriate since the current replaces a southward component with a sunward component (giving a $\sqrt{2}$ factor) and the current flows diagonally across the side of the magnetosphere (giving another $\sqrt{2}$ factor). Thus for the $B_z = -30$ nT run, $I_s = 4.6$ MA or about twice I_f . This qualitative result based on dimensional analysis compares favorably with the MHD simulation, which finds a total region 1 current equal to about twice the 3.5 MA computed for the Chapman-Ferraro current.

[26] To summarize, in the saturation domain the total current flowing in the region 1 current system is limited by the amount of current needed to stop and deflect the solar wind (I_f) plus the amount of current needed to shear the reconnected solar wind field parallel to the solar wind flow (I_s). Once the transpolar potential imposed by magneto-

pause reconnection draws this much current, it has reached a limit. There is no way to close any more current in the region 1 system in the interaction between the solar wind and the magnetosphere. This seems to be the scenario that the MHD runs are describing.

6. Relation Between Transpolar Potential Saturation and Magnetospheric Erosion

[27] Usurpation of Chapman-Ferraro current by the region 1 current system as the interplanetary electric field increases shows up in an interesting way that results from the region 1 current system generating magnetic field at the subsolar magnetopause that is oppositely directed to the dipole field there. Whereas the Chapman-Ferraro current system strengthens the field at the subsolar magnetopause, the region 1 current system weakens it.

[28] Figure 5 displays results from a number of ISM runs to illustrate this effect. The ordinate in the graph shows the amount by which the magnetic field on the magnetospheric side of the subsolar point is stronger than the dipole field there. This absolute difference is normalized by dividing by the dipole term. For instance, according to analytical solutions of the vacuum Chapman-Ferraro problem [e.g., Mead, 1964], the total field strength at the subsolar point is ~ 70 nT where the dipole strength is ~ 30 nT. The value of the ordinate on the graph in this case would be $4/3$ or 1.3 .

[29] The first point in the graph at a value of 1.2 , obtained for a strictly northward IMF, represents a nearly pure Chapman-Ferraro situation. The next two points in the graph were obtained for IMF clock angles (as seen from the Sun) of 45° and 90° , respectively. The remaining four points come from the four runs described in section 2. The dashed line is just to help the eye bridge the gaps between points. The horizontal line at the value zero divides situations above where the Chapman-Ferraro current is still strong enough to compress the field at the subsolar point from situations below where the region 1 current has invaded to the point of dominance. Note that for IEFs greater than ~ 3 mV/m, the magnetospheric magnetic field at the subsolar point is weaker than the dipole field there.

[30] Cahill and Winckler [1999, Figure 3] report just such a case in a study of magnetopause crossing by geosynchronous satellites. Data from GOES 6 and 7 near noon during a magnetic storm on 8 November 1991 show that when the magnetopause passed over the satellites the field strength was less than the dipole field. Moreover, there is indirect evidence that Chapman-Ferraro dynamics is replaced by region 1 system dynamics when the IMF points southward. Russell *et al.* [1994] reports that low-latitude sudden impulses are weaker for the same jump in ram pressure when the IMF is southward compared with when it is northward. Russell *et al.* attribute the difference to an enhancement of the tail current, but it could also be simply that the compression effect of the Chapman-Ferraro current is reduced by the region 1 current system.

[31] This is perhaps an appropriate place to address a point of possible confusion concerning the relation between "magnetospheric erosion" (the habit of the dayside magnetopause to move earthward when the IMF turns southward first noted by Fairfield [1971] and now explicitly incorporated in empirical magnetopause-position models

(e.g., most recently Shue *et al.* [1998])) and the weakening of the magnetic field at the dayside magnetopause by the region 1 current system, which we have been discussing. These are different expressions of the same thing. It is the weakening of the magnetic field at the dayside magnetopause by the region 1 current system that causes the magnetopause to move Earthward so that it can reach a point at which the magnetic pressure again balances the ram pressure. (The tail current system weakens the field, too, but being farther away its contribution is less.) Earthward motion of the magnetopause when the current flowing in the region 1 current system increases is inevitable since ram pressure must at all times be balanced at the stagnation point. The magnetopause moves Earthward (the direction of stronger dipole field) in order to hold the field strength at the stagnation point constant in the face of weakening of the field that as shown in Figure 5, the region 1 current system effects. "Magnetospheric erosion" is just a metaphor that we have traditionally adopted to describe this process of reactive magnetostasis.

7. Summary

[32] Observations seem to be consistently revealing that when the motional electric field of the solar wind (the IEF) exceeds roughly 3 mV/m, the transpolar potential stops rising linearly with IEF. Instead it flattens out and as the IEF grows more, reaches some upper limit called the saturation potential, which is typically 150 to 250 kV. Thomas Hill predicted this behavior and gave a conceptual framework in which it could be modeled analytically. Subsequently, MHD simulations exhibited the saturation phenomenon in good accord with the Hill model. This paper gives an explicit demonstration of saturation in both the Hill model and MHD simulations and documents their correspondence.

[33] The MHD simulations, as shown here, further suggest that transpolar potential saturation results not from a limit on reconnection but from solar wind ram pressure limiting the amount to which the total region 1 current can grow. (In the saturation domain of IEF, the region 1 current system usurps the position of Chapman-Ferraro currents.) Thus saturation of transpolar potential is a manifestation of region 1 current limitation by ram pressure.

[34] **Acknowledgments.** The work was supported by grants from NSF's Upper Atmospheric Section of the Atmospheric Sciences Division and NASA's SR&T and Sun-Earth Connections Theory Programs. The Integrated Space Weather Model was developed by Mission Research Corporation under contract from the Defense Threat Reduction Agency, Willard White principal investigator. Daniel Weimer developed the graphics package (ISM_VIEW) used to generate the images.

[35] Arthur Richmond thanks John G. Lyon and another reviewer for their assistance in evaluating this paper.

References

- Burke, W. J., D. R. Weimer, and N. C. Maynard, Geoeffective interplanetary scale sizes derived from regression analysis of polar cap potentials, *J. Geophys. Res.*, **104**, 9989–9994, 1999.
- Cahill, L. J., Jr., and J. R. Winckler, Magnetopause crossings observed at $6.6 R_E$, *J. Geophys. Res.*, **104**, 12,229–12,237, 1999.
- Coroniti, F. V., and C. F. Kennel, Magnetospheric reconnection, substorms, and energetic particle acceleration, in *Particle Acceleration in Planetary Magnetospheres*, edited by J. Arons, C. Max, and C. McKee, pp. 169–178, Am. Inst. of Phys., New York, 1979.
- Crooker, N. U., and G. L. Siscoe, On the limits of energy transfer through dayside merging, *J. Geophys. Res.*, **91**, 13,393–13,397, 1986.

- Fairfield, D. H., Average and unusual locations of the Earth's magnetopause and bow shock, *J. Geophys. Res.*, *76*, 6700–6716, 1971.
- Fedder, J. A., and J. G. Lyon, The solar wind-magnetosphere-ionosphere current-voltage relationship, *Geophys. Res. Lett.*, *14*, 880–883, 1987.
- Hain, K., The partial donor cell method, *J. Comp. Physics*, *73*, 131, 1987.
- Hill, T. W., Magnetic coupling between solar wind and magnetosphere: Regulated by ionospheric conductance?, *Eos Trans. AGU*, *65*, 1047–1048, 1984.
- Hill, T. W., A. J. Dessler, and R. A. Wolf, Mercury and Mars: The role of ionospheric conductivity in the acceleration of magnetospheric particles, *Geophys. Res. Lett.*, *3*, 429–432, 1976.
- Iijima, T., and T. A. Potemra, The amplitude distribution of field-aligned currents at northern high latitudes observed by Triad, *J. Geophys. Res.*, *81*, 2165–2174, 1976.
- Mead, G. D., Deformation of the geomagnetic field by the solar wind, *J. Geophys. Res.*, *69*, 1181–1195, 1964.
- Reiff, P. H., R. W. Spiro, and T. W. Hill, Dependence of polar cap potential drop on interplanetary parameters, *J. Geophys. Res.*, *86*, 7639–7648, 1981.
- Reiff, P. H., and J. G. Luhmann, Solar wind control of the polar-cap voltage, in *Solar Wind - Magnetosphere Coupling*, edited by Y. Kamide and J. A. Slavin, pp. 453–476, Terra Sci., Tokyo, 1986.
- Russell, C. T., M. Ginsky, and S. M. Petrinc, Sudden impulses at low latitude stations: Steady state response for southward interplanetary magnetic field, *J. Geophys. Res.*, *99*, 13,403–13,408, 1994.
- Russell, C. T., G. Lu, and J. G. Luhmann, Lessons from the ring current injection during the September 24, 25, 1998 storm, *Geophys. Res. Lett.*, *27*, 1371–1374, 2000.
- Russell, C. T., J. G. Luhmann, and G. Lu, Nonlinear response of the polar ionosphere to large values of the interplanetary electric field, *J. Geophys. Res.*, *106*, 18,496–18,504, 2001.
- Sanchez, E. R., and G. L. Siscoe, IMP 8 magnetotail boundary crossings: A test of the MHD models for an open magnetopause, *J. Geophys. Res.*, *95*, 20,771–20,779, 1990.
- Sanchez, E. R., G. L. Siscoe, and C.-I. Meng, Inductive attenuation of the transpolar voltage, *Geophys. Res. Lett.*, *18*, 1173–1176, 1991.
- Shue, J.-H., et al., Magnetopause location under extreme solar wind conditions, *J. Geophys. Res.*, *103*, 17,691–17,000, 1998.
- Siebert, K. D., and G. L. Siscoe, Dynamo circuits for magnetopause reconnection, *J. Geophys. Res.*, *107*, 10.1029/2001JA000237, 2002.
- Siscoe, G. L., G. M. Erickson, B. U. Ö. Sonnerup, N. C. Maynard, J. A. Schoendorf, K. D. Siebert, D. R. Weimer, W. W. White, and G. R. Wilson, Hill model of transpolar potential saturation: Comparisons with MHD simulations, *J. Geophys. Res.*, *107*, 10.1029/2001JA000109, 2002.
- Weimer, D. R., An improved model of ionospheric electric potentials including substorm perturbations and application to the Geospace Environment Modeling November 24, 1996 event, *J. Geophys. Res.*, *106*, 407–416, 2001.
- White, W. W., J. A. Schoendorf, K. D. Siebert, N. C. Maynard, D. R. Weimer, G. L. Wilson, B. U. Ö. Sonnerup, G. L. Siscoe, and G. M. Erickson, MHD Simulation of magnetospheric transport at the mesoscale, *Space Weather, Geophys. Monogr. Ser.*, vol. 125, edited by P. Song, H. J. Singer, and G. L. Siscoe, pp. 229–240, AGU, Washington, D.C., 2001.
- Wygant, J. R., R. B. Torbert, and F. S. Mozer, Comparison of S3-3 polar cap potential with the interplanetary magnetic field and models of magnetospheric reconnection, *J. Geophys. Res.*, *88*, 5727–5735, 1983.
- Zesta, E., H. J. Singer, D. Lummerzheim, C. T. Russell, L. R. Lyons, and M. J. Brittnacher, The effect of the January 10, 1997, pressure pulse on the magnetosphere-ionosphere current system, in *Magnetospheric Current Systems, Geophys. Monogr. Ser.*, vol. 118, edited by S.-I. Ohtani et al., pp. 217–226, AGU, Washington, DC, 2000.

N. U. Crooker and G. L. Siscoe, Center for Space Physics, Boston University, 725 Commonwealth Ave., Boston, MA 02215, USA. (crooker@bu.edu; siscoe@bu.edu)

K. D. Siebert, Mission Research Corporation, 589 West Hollis St., Suite 201, Nashua, NH 03062, USA. (ksiebert@mrcnh.com)

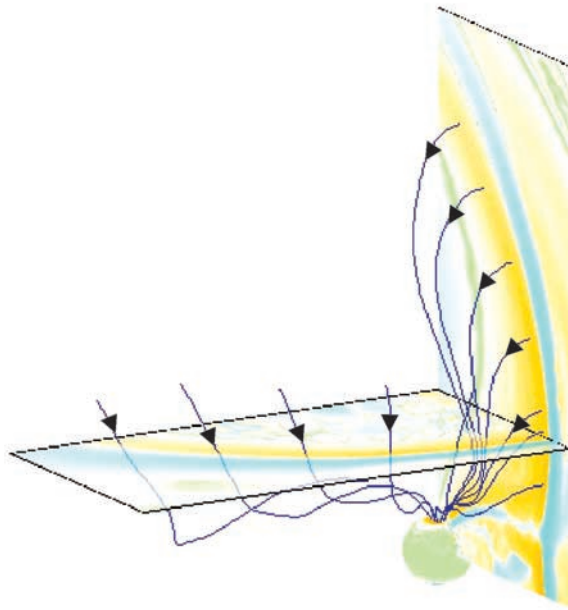


Figure 4. Three-dimensional view generated from the simulation having maximum IEF. Current flowlines were initiated in the tan layer, representing the magnetopause. Shading denotes radial component of the $\mathbf{J} \times \mathbf{B}$ force (tan is outward directed force and blue is inward directed force).